The Dimerization of TiH_4

Simon P. Webb and Mark S. Gordon*

Contribution from the Department of Chemistry, Iowa State University, Ames, Iowa 50011

Received February 17, 1995[⊗]

Abstract: *Ab initio* electronic structure calculations using a triple-ζ plus polarization basis set, second-order perturbation theory, and coupled cluster theory show the dimerization of TiH_4 to be kinetically and thermodynamically very favorable. Six minima have been found on the potential energy surface of Ti_2H_8: two with double hydrogen bridges and four with triple hydrogen bridges. This potential energy surface is very flat suggesting rapid interconversion between these isomers is possible. The large thermodynamic driving force for dimerization (up to −46.1 kcal/mol on the classical surface) is attributed to both electrostatic effects and the electron deficiency of titanium.

I. Introduction

During recent years there has been a significant increase in the number of experimental studies of transition metal hydrides. This is indicative of increasingly sophisticated techniques such as low-temperature matrix isolation,[1] which facilitate study of these often highly unstable but important compounds. Theory has a vital role to play both in interpretation of experiment and as a predictive tool; however, adequate *ab initio* calculations on transition metal hydrides have proved challenging. It seems then, that careful systematic theoretical investigation of the simplest transition metal hydrides is necessary as a foundation for work on more complex systems.

This work is highly desirable in view of the fact that molecular species containing Ti−H bonds are rich with exciting chemistry but are often not well characterized or understood.[2] Their role as catalysts in reactions such as hydrosilation[3] and polymerization of olefins[4] is of particular interest. The ability of some of these compounds to reduce molecular nitrogen has been demonstrated;[4b,5] obviously, successful modification of these species to facilitate a catalytic role in this reaction would be of tremendous importance, but difficult without a solid understanding of basic titanium hydride chemistry.

There have been a number of theoretical studies on TiH_2[6] and on the titane molecule TiH_4.[7] These studies of simple titanium hydrides have yielded fundamental and pertinent information on the nature of Ti−H bonding. Only two experimental studies of TiH_4 have been found in the literature: the formation of TiH_4 from the decomposition of a $TiCl_4$−H_2 mixture at low pressures in 1963 by Breisacher and Siegel,[8] and a low-temperature matrix study of the reaction between naked Ti atoms and H_2.[9] In the latter, the reaction products have been characterized by infrared spectroscopy. The spectra are complex with broad features making interpretation difficult.

A number of titanium hydrides are known to exist as dimers with bridging hydrogens.[2,10] Titanium is also known to form hydrogen bridging bonds with other elements,[2,11] for example in $(\eta^5\text{-}C_5H_5)_2TiBH_4$ titanium is bonded to boron through a double hydrogen bridge. A thorough understanding of the simplest titanium hydride dimers will be useful when considering the many transition metal species containing similar three center, two electron bonding arrangements.

Titanium has valence electron configuration $4s^23d^2$ compared to $2s^22p^2$ and $3s^23p^2$ of its highly studied group IVA analogs carbon and silicon. A recent study[12] has explored the impact of the differences between the s^2d^2 and s^2p^2 electronic configurations of these elements on the structures they form. In this paper we continue this exploration. It is well-known that the saturated molecules CH_4 and SiH_4 show no propensity to dimerize; however, this is not the case for TiH_4. We report here results of a detailed *ab initio* analysis of the potential energy surface of the isomers of Ti_2H_8 which show that the dimerization of TiH_4 is thermodynamically and kinetically very favorable. Calculated infrared frequencies are also reported for comparison with experiment.[9]

II. Computational Methods

Preliminary calculations were performed on TiH_4 and Ti_2H_8 using multi-configurational SCF (MCSCF) wave functions and Huzinaga's 21 split valence basis set.[13] For TiH_4 an 8 electron, 8 orbital active space was used for geometry optimization. This includes all valence electrons and allows all Ti−H bonds to be correlated. A natural orbital analysis shows that the maximum occupation of any virtual orbital is 0.07 electron, with a total of only 3.1% of the 8 valence electrons outside the closed shell configuration. For Ti_2H_8 a full valence 16 electron, 16 orbital MCSCF active space is beyond our capabilities; however, a smaller well-chosen active space was thought sufficient to establish the nature of the wave function. Therefore, we elected to carry out a single-point singles and doubles configuration interaction (CI) calculation at the RHF geomery using the 16 valence electrons (8 RHF orbitals) as a reference, with excitation into all virtual orbitals. A

[⊗] Abstract published in *Advance ACS Abstracts,* June 15, 1995.

(1) Sweeny, R. L. In *Transition Metal Hydrides*; Dedieu, A., Ed.; VCH Publishers Inc.: New York, 1992; pp 65−101.

(2) Toogood, G. E.; Wallbridge, M. G. H. *Adv. Inorg. Chem. Radiochem.* **1982** *25*, 267.

(3) Barton, T. J.; Boudjouk, P. *Organosilican Chemistry—A Brief Overview*; Advances in Chemistry; Ziegler, J., Ed.; American Chemical Society: Washington, DC, 1990.

(4) (a) Pez, G. P. *J. Chem. Soc., Chem. Commun.* **1977**, 560. (b) Pez, G. P.; Kwan, S. C. *J. Am. Chem. Soc.* **1976**, *98*, 8079.

(5) Bercaw, J. E.; Marvich, R. H.; Bell, L. G.; Brintzinger, H. H. *J. Am. Chem. Soc.* **1972**, *94*, 1219.

(6) (a) Kudo, T.; Gordon, M. S. *J. Chem. Phys.* **1995**, *102*, 6806. (b) Demuynk, J.; Schaefer, H. F. *J. Chem. Phys.* **1980**, *72*, 311. (c) Tyrrell, J.; Youakim, A. *J. Phys. Chem.* **1980**, *84*, 3568. (d) Tyrrell, J.; Youakim, A. *J. Phys. Chem.* **1981**, *85*, 3614.

(7) Thomas, J. R.; Quelch, G. E.; Seidl, E. T.; Schaefer, H. F. *J. Chem. Phys.* **1992**, *96*, 6857 and references therein.

(8) Breisacher, A.; Siegel, B. *J. Am. Chem. Soc.* **1963**, *85*, 1705.

(9) Xiao, Z. L.; Hauge, R. H.; Margrave, J. L. *J. Phys. Chem.* **1991**, *95*, 2696.

(10) (a) Gauvin, F.; Britten, J.; Samuel, E.; Harrod, J. F. *J. Am. Chem. Soc.* **1992**, *114*, 1489. (b) Cristol, S. J.; Ziebarth, T. D.; Turro, N. J.; Stone, P.; Scribe, P. *J. Am. Chem. Soc.* **1974**, *96*, 3017; (c) Britzinger, H. H.; Bercaw, J. E. *J. Am. Chem. Soc.* **1970**, *92*, 6182.

(11) Marks, T. J.; Jolb, J. R. *Chem. Rev.* **1977**, *77*, 263.

(12) Kudo, T.; Gordon, M. S. *J. Phys. Chem.* In press.

(13) Huzinaga, S.; Andzelm, J.; Klobukowski, M.; Radzio-Andzelm, E.; Sakai, Y.; Tatewaki, H.; In *Gaussian Basis Sets for Molecular Calculations*; Elsevier: Amsterdam, 1984.

0002-7863/95/1517-7195$09.00/0

Table 1. Calculated Total Energies (in Hartrees) of the Titane Molecule, and Zero-Point Vibrational Energy Correction at the MP2/TZVP Level

point group	TZVP				TZVP(f)	
	RHF(opt)	MP2(opt)	CCSD(T)[a]	Z.P.E.$_{(MP2)}$	CCSD(T)[a]	ΔH(CCSD(T))[b]
T_d	−850.59992	−850.73823	−850.77402	0.02212	−850.79274	−850.77062

[a] All single-point energies calculated at the MP2/TZVP optimized geometry. [b] ΔH(CCSD(T)) value is the single-point CCSD(T)/TZVP(f) energy with zero-point vibrational energy added.

natural orbital analysis of this CI wave function was then used to choose the 12 "most active" natural orbitals. These were then used as a starting point for a 12 electron, 12 orbital MCSCF calculation. A natural orbital analysis of the resulting MCSCF wave function revealed the largest occupation of the virtual orbitals to be 0.12 and 0.11; again only 3.1% of the active space electrons are outside the closed shell configuration. It is therefore concluded that the single determinant Hartree−Fock self consistent field (SCF) wave function is an adequate reference for the system under investigation.

Then for titanium a triple-ζ with polarization (14s11p6d/10s8p3d) basis was employed which consists of Wachter's basis set[14] with two additional p functions[15] and a diffuse d function.[16] For hydrogen, Dunning's basis set[17] (5s1p/3s1p) was used. Collectively this basis set for titanium and hydrogen will be referred to as TZVP. For final single-point energies one set of f functions ($\alpha_f = 0.4$)[18] was added to the titanium basis. This basis set will be referred to as TZVP(f).

Geometry optimizations were carried out at the RHF and second-order perturbation theory (MP2[19]) levels. Stationary points were characterized as minima or transition states by calculating and diagonalizing the matrix of the energy second derivatives (hessian). Single-point energies were calculated at the coupled cluster (CCSD(T)[20]) level of theory, with final CCSD(T) calculations employing the TZVP(f) basis set. All RHF and MCSCF calculations were done using GAMESS;[21] the MP2 and CCSD(T) calculations were done using GAUSSIAN 92.[22]

III. Results and Discussion

TiH_4. Both RHF and MP2 predict TiH_4 to be tetrahedral, with a Ti−H bond length of 1.70 Å (Figure 1). These are in good agreement with the results of Schaefer and Thomas.[7] The total energies (given in Table 1) and bond lengths of TiH_4 will be used as a baseline against which Ti_2H_8 isomers can be compared.

Ti_2H_8. The geometries for the double hydrogen bridged (μ-H)$_2$ and triple hydrogen bridged (μ-H)$_3$ minima on the Ti_2H_8 potential energy surface are shown in Figure 2. Attempts were made to find (μ-H)$_4$ bridged structures; however, no such structures were found. Before considering the (μ-H)$_2$ and (μ-H)$_3$ bridged structures explicitly, we discuss the pathways leading from $TiH_4 + TiH_4 \rightarrow Ti_2H_8$.

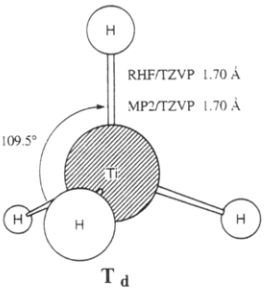

Figure 1. Titane equilibrium geometry.

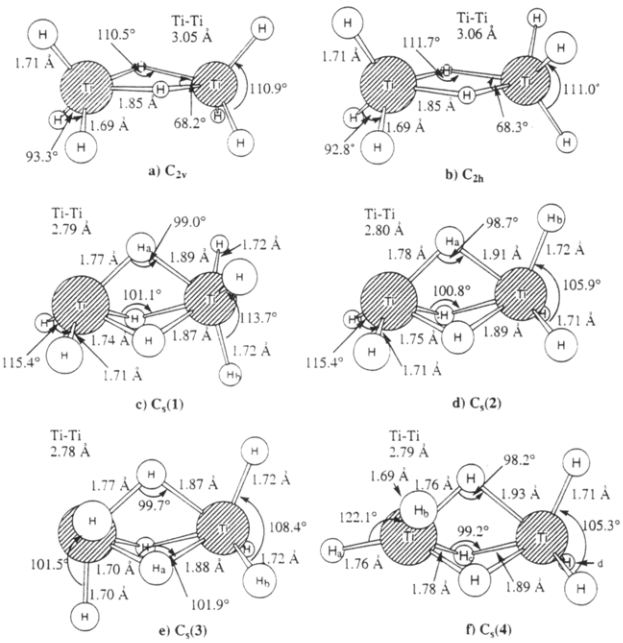

Figure 2. MP2/TZVP optimized structures which are minima on the potential energy surface of Ti_2H_8. In $C_s(1)$, $C_s(2)$, and $C_s(3)$ the two Ti's, H_a, and H_b are in the plane. In $C_s(4)$ The two Ti's, H_a, H_b, H_c, and H_d are in the plane.

(a) Constrained Optimizations. Continuous "downhill" paths to dimerization were found via a series of constrained geometry optimizations at the RHF/TZVP level, followed by MP2/TZVP single-point energy calculations. These constrained optimizations were carried out by starting from the RHF/TZVP optimized minima of interest, increasing the Ti−Ti separation in small intervals, and at each interval keeping this Ti−Ti separation fixed while minimizing the energy with respect to all other bond lengths and angles.

Plots of the MP2/TZVP single-point energies versus the Ti−Ti separation which correspond to dissociating the dimers $C_s(1)$ (Figure 2c) and $C_s(4)$ (Figure 2f) can be seen in Figure 4a and Figure 4b, respectively. The reverse of this separation process is a path to dimerization. Structures along these dimerization paths can be seen in Figures 5a and 5b. In Figure 5a the two TiH_4 fragments approach each other in a staggered conformation. A hydrogen on one TiH_4 (which has a partial negative charge) points directly at the titanium on the other TiH_4 (which has a partial positive charge) and so an attractive interaction

(14) Watchters, A. J. H. *J. Chem. Phys.* **1970**, *52*, 1033.
(15) Hood, D. M.; Pitzer, R. M.; Schaefer, H. F. *J. Chem. Phys.* **1979**, *71*, 705.
(16) Rappe, A. K.; Smedley, T. A.; Goddard, W. A. *J. Phys. Chem.* **1981**, *85*, 2607.
(17) Dunning, T. H.; Hay, P. J. In *Methods of Electronic Structure Theory*; Schaefer, H. F., III, Ed.; Plenum Press: New York, 1977; pp 1−27.
(18) This choice of exponent is based on energy optimizations for several small Ti-containing compounds and on discussions with Dr. Charles W. Bauschlicher, Jr.
(19) (a) Binkley, J. S.; Pople, J. A. *Int. J. Quantum Chem.* **1975**, *9*, 229. (b) Krishnan, R.; Pople, J. A. *Int. J. Quantum Chem.* **1978**, *14*, 91.
(20) Pople, J. A.; Head-Gordon, M.; Raghavachari, K. *J. Chem. Phys.* **1987**, *87*, 5968.
(21) Schmidt, M. W.; Baldridge, K. K.; Boatz, J. A.; Jenson, J. H.; Koseki, S.; Matsunaga, N.; Gordon, M. S.; Ngugen, K. A.; Su, S.; Windus, T. L.; Elbert, S. T.; Montgomery, J.; Dupuis, M. *J. Comp. Chem.* **1993**, *14*, 1347.
(22) Frisch, M. J.; Trucks, G. W.; Head-Gordon, M.; Gill, P. M. W.; Wong, M. W.; Foresman, J. B.; Johnson, B. G.; Schlegel, H. B.; Robb, M. A.; Replogle, E. S.; Gomperts, R.; Andres, J. L.; Raghavachari, K.; Binkley, J. S.; Gonzalez, C.; Martin, R. L.; Fox, D. J. DeFrees, D. J.; Baker, J.; Stewe t, J. J. P.; Pople, J. A. *GAUSSIAN92*; GAUSSIAN, INC.; Pittsburgh, PA, 1992.

Table 2. Calculated Energies (in kcal mol^{-1}) of Ti_2H_8 Relative to $2TiH_4$ and Zero-Point Energy Corrections at the MP2/TZVP Level

	TZVP				TZVP(f)	
	RHF(opt)	MP2(opt)	CCSD(T)[a]	Z.P.E.(MP2)	CCSD(T)[a]	ΔH(CCSD(T))[b]
			minima			
C_{2v}	−23.0	−37.1	−36.8	3.0	−37.2	−34.2
C_{2h}	−23.2	−37.4	−36.9	3.0	−37.4	−34.4
$C_s(1)$	−20.7	−45.5	−41.6	5.2	−43.8	−38.6
$C_s(2)$	−20.7	−46.9	−43.2	5.4	−46.1	−40.7
$C_s(3)$		−43.6	−38.9	5.2	−41.1	−35.9
$C_s(4)$		−43.9	−41.3	4.4	−43.2	−38.8
			transition states			
T.S.(1)		−37.1	−36.7	2.8	−37.2	−34.4
T.S.(2)		−35.5	−34.6	2.9	−35.5	−32.6
T.S.(3)		−45.5	−41.6	2.2	−43.9	−41.7
T.S.(4)		−43.6	−38.9	5.1	−41.2	−36.1
T.S.(5)		−43.9	−41.3	4.3	−43.2	−38.9

[a] All single-point energies calculated at the MP2/TZVP optimized geometry. [b] ΔH(CCSD(T)) values are the single-point CCSD(T)/TZVP(f) energies with zero-point vibrational energies added.

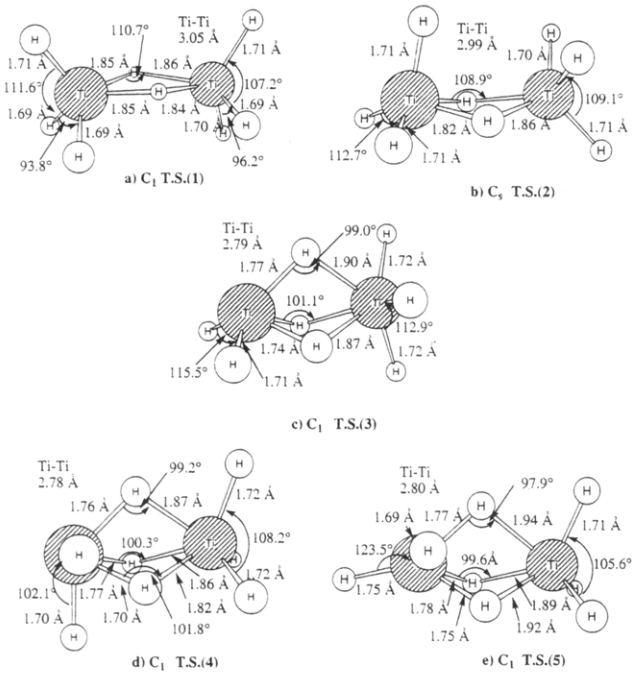

Figure 3. MP2/TZVP optimized structures which are transition states on the potential energy surface of Ti_2H_8.

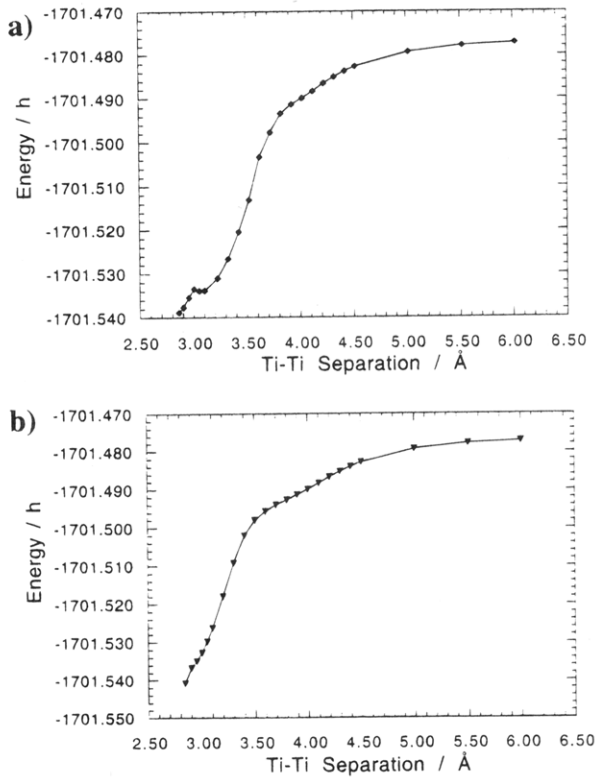

Figure 4. Plots of MP2/TZVP single-point energies in hartrees versus Ti−Ti separation in Å corresponding to (a) the dissociation of $C_s(1)$ (Figure 2c) into two TiH_4 fragments and (b) the dissociation of $C_s(4)$ (Figure 2f) into two TiH_4 fragments. The single-point energies were calculated at the constrained RHF/TZVP optimized geometries (Ti−Ti distance constrained).

occurs. It can be seen from Figure 4a that this initial interaction and the subsequent formation of a second bridging bond continuously lowers the energy until a $(\mu\text{-H})_2$ minimum is reached at Ti−Ti ~3.10 Å. A small barrier to formation of the lower energy $(\mu\text{-H})_3$ structure is then encountered. The situation in Figure 5b is somewhat different. Here the two TiH_4 fragments approach each other in an eclipsed conformation. Again the initial interaction is between a hydrogen from one TiH_4 and the titanium from the other TiH_4. Then two other hydrogens form bridging bonds simultaneously and a $(\mu\text{-H})_3$ structure is formed directly. Figure 4b shows this process lowers the energy continuously.

It is important to note that although these paths to dimerization are probably not the only ones and may not be the lowest energy paths, as the geometries are not optimized at a correlated level of theory, they do establish the fact that dimerization can occur with no barrier.

(b) Minima and Transition States. MP2/TZVP bond lengths and angles are shown in Figure 2 for all minima and Figure 3 for all transition states. Energies are given in Table 2.

Two $(\mu\text{-H})_2$ isomers were discovered: a C_{2v} structure with eclipsed terminal hydrogens (Figure 2a) and a C_{2h} structure with staggered terminal hydrogens (Figure 2b). The Ti−H bond length for the terminal hydrogens in these structures is very similar to that found in the monomeric TiH_4; however, for the bridging hydrogens the Ti−H distance is lengthened considerably (0.15 Å). This is consistent with the findings for other cases of 3 center, 2 electron bonding such as the prototypical B_2H_6.[23a] The two isomers are essentially isoenergetic (Table 2). This may be explained by the large separation of terminal hydrogens on one titanium center from those on the other, thus avoiding the hydrogen−hydrogen interactions which affect the

(23) (a) Shen, M.; Schaefer, H. F. *J. Chem. Phys.* **1992**, *96*, 2868. (b) Cioslowski, J.; McKee, M. L. *J. Phys. Chem.* **1992**, *96*, 9264.

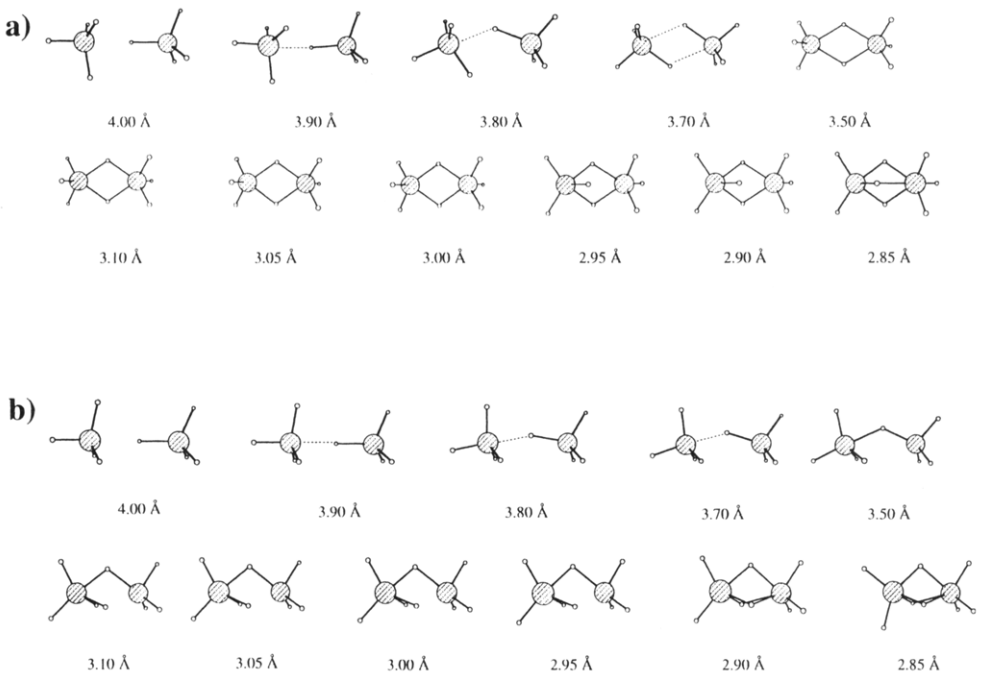

Figure 5. Each structure is the result of a constrained optimization at the RHF/TZVP level in which the Ti−Ti separation was "frozen" at the distance indicated: (a) represents a possible dimerization path to $C_s(1)$ (Figure 2c), and (b) represents a possible dimerization path to $C_s(4)$ (Figure 2f).

relative stabilities of (for example) staggered and eclipsed ethane. Interconversion of these $(\mu\text{-H})_2$ isomers proceeds via the transition state T.S.(1) (Figure 3a) with effectively no barrier (see Table 2 and Figure 6) suggesting totally free rotation. The internal rotation in $(\mu\text{-H})_2\ Ti_2H_8$ may be represented schematically as follows:

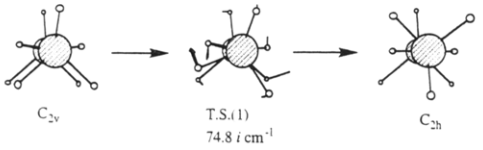

The absence of a barrier to rotation may be explained by the large distances between vicinal hydrogens and by the availability of d orbitals which facilitate isoenergetic bonding for any rotational arrangement of the terminal hydrogens. Formation of both these dimers is exothermic relative to the separated monomers by ~37 kcal/mol on the classical potential energy surface (Table 2 and Figure 6a) and by ~34 kcal/mol on the adiabatic ground state surface (zero-point vibrational energy included) (Table 2 and Figure 6b) at the CCSD(T)/TZVP(f) level of theory. It may be noted (as it has been previously[23a]) that dynamic electron correlation plays a vital role in the quantitative description of three center, two electron bonding. The dimerization energy of TiH_4 is ~14 kcal/mol more exothermic at all correlated levels of theory than at the RHF/TZVP level of theory.

Four $(\mu\text{-H})_3$ isomers with C_s symmetry were found: $C_s(1)$, $C_s(2)$, $C_s(3)$, and $C_s(4)$ corresponding to Figure 2c,d,e,f. These four C_s isomers differ primarily in the orientation of their terminal hydrogens. All four of these structures are several kilocalories per mole lower in energy than the $(\mu\text{-H})_2$ isomers, with $C_s(2)$ appearing to be the global minimum. Transition state T.S.(2) (Figure 3b) connects the $(\mu\text{-H})_2$ C_{2h} isomer (Figure 2b) with the $(\mu\text{-H})_3$ $C_s(1)$ isomer (Figure 2c), as shown schematically below.

The energy barrier for this process (Table 2 and Figure 6) is 1.9 and 1.8 kcal/mol on the classical and adiabatic ground state

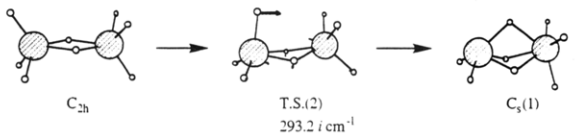

potential energy surfaces, respectively. The reverse barriers are 8.3 and 6.0 kcal/mol for the classical and the adiabatic ground state surfaces, respectively.

The $(\mu\text{-H})_3$ structures are local minima corresponding to different rotational orientations of their terminal hydrogens. It is evident from Figure 6 that the potential energy surface connecting these isomers is quite flat and rapid interconversion should be possible via transition states T.S.(3), T.S.(4), and T.S.-(5) (Figures 3c,d,e), as shown below for the MP2 surface.

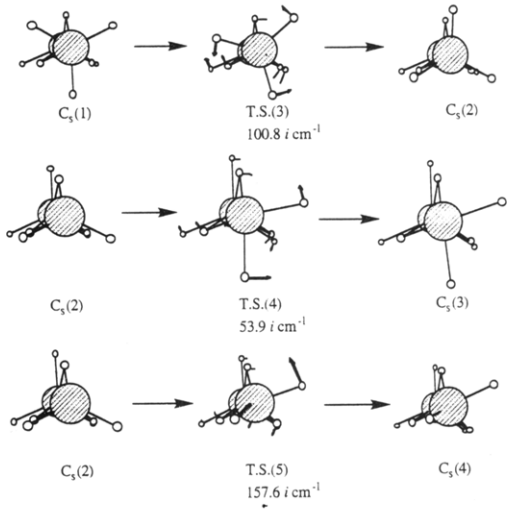

Again, this flat surface is indicative of the ability of d orbitals to form bonds with similar energy for a range of terminal hydrogen positions.

Figure 6 shows that the $(\mu\text{-H})_3$ isomers are even more stable relative to the separated monomers than their $(\mu\text{-H})_2$ counter-

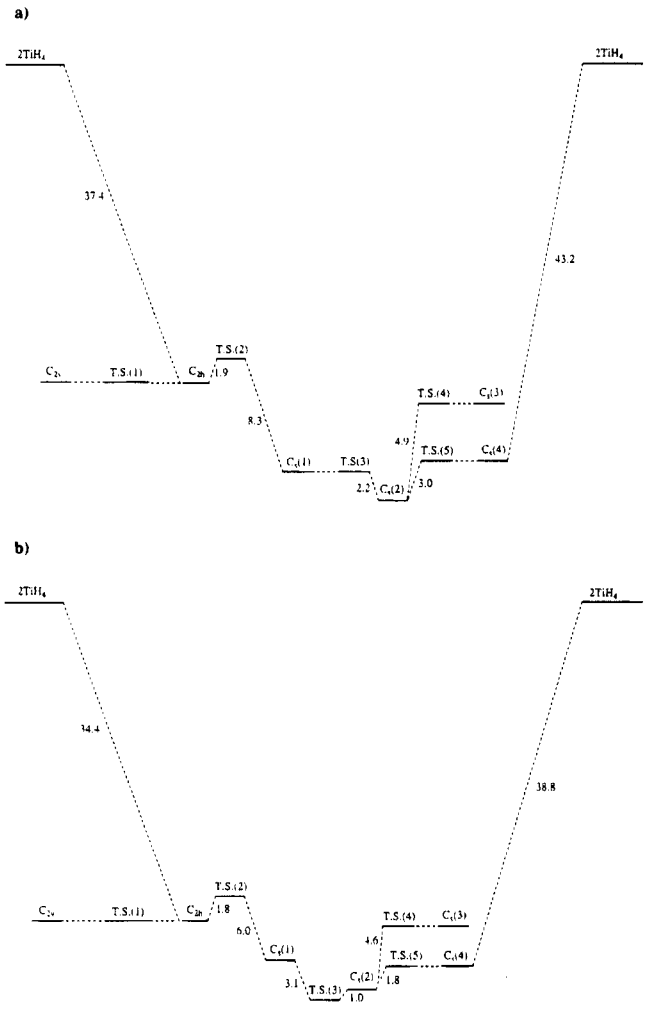

Figure 6. (a) CCSD(T)/TZVP(f) potential energy surface for Ti_2H_8. (b) CCSD(T)/TZVP(f) potential energy surface for Ti_2H_8 with zero-point vibrational energy (calculated at the MP2/TZVP level) added. All energies are in kcal mol^{-1} (diagrams not to scale).

parts, $C_s(2)$ (the global minimum) being 46.1 kcal/mol more stable than $2TiH_4$ on the classical surface at the CCSD(T)/TZVP(f) level of theory. This can be attributed to the extra stabilizing effect of the third bridging bond, and titanium's desire for high coordination numbers. Dynamic correlation again plays an important role in describing the bridging bonds. At the RHF/TZVP level the $(\mu\text{-H})_3$ isomers are in fact *higher* in energy than the $(\mu\text{-H})_2$ isomers. This reversal in the relative stabilities of the $(\mu\text{-H})_2$ and $(\mu\text{-H})_3$ isomers is due to the effects of dynamic electron correlation. Even using MP2/TZVP single-point energies at RHF/TZVP geometries, the $(\mu\text{-H})_3$ $C_s(1)$ isomer is 5.9 kcal/mol more stable than the $(\mu\text{-H})_2$ C_{2h} isomer. The $C_s(1)$ isomer is stabilized by a further 2.2 kcal/mol relative to the C_{2h} isomer with the contraction of its three center bonds on MP2 geometry optimization.

Because the potential energy surface in the $(\mu\text{-H})_3$ region is so flat, single-point energy calculations at higher levels of theory and incorporation of vibrational zero-point corrections reverses the order of several stationary points. Indeed, at the CCSD(T)/TZVP(f) + ZPE level of theory, T.S.(3) drops 1 kcal/mol below $C_s(2)$. So, very high levels of theory and anharmonic vibrational effects are needed to obtain a highly accurate representation of the $(\mu\text{-H})_3$ bridging region of the surface. Nonetheless, it is clear that in general, the dimerization of $2TiH_4$ to Ti_2H_8 is highly exothermic.

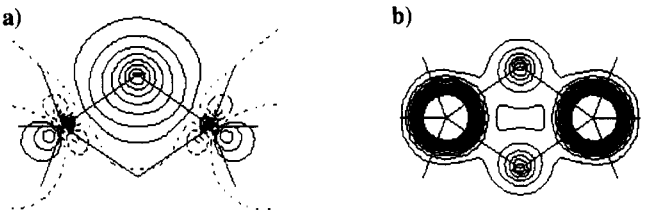

Figure 7. (a) Localized molecular orbital corresponding to a three-center, two-electron hydrogen bridging bond in the C_{2h} isomer. (b) Plot of total electron density for the C_{2h} isomer. The contour increments in (a) and (b) are 0.05 $bohr^{3/2}$ and $bohr^3$, respectively.

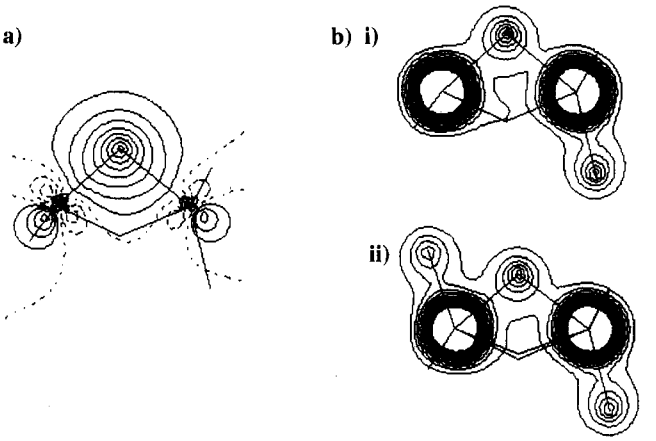

Figure 8. (a) Localized molecular orbital corresponding to the in-plane three-center, two-electron hydrogen bridging bond in the $C_s(1)$ isomer. (b) Plot of total electron density in the C_s plane of the $C_s(1)$ isomer (i) and plot of the total density in the plane of one of the remaining bridging hydrogens of the $C_s(1)$ isomer (ii). Contour increments in (a) and (b) are 0.05 $bohr^{3/2}$ and $bohr^3$, respectively.

(c) Bonding in Ti_2H_8. In order to gain some insight into the nature of the bonding in these Ti_2H_8 isomers, particularly the three center bonds, the RHF/TZVP molecular orbitals of two minima, C_{2h} (Figure 2b) and $C_s(1)$ (Figure 2c) at their MP2/TZVP geometries, were localized using the method of Edmiston and Ruedenberg.[24] In addition, Mulliken populations and charges were calculated using the MP2 density to give some indication of the degree of polarity in the bonds.

None of the localized molecular orbitals for either of the two structures show any direct σ titanium−titanium interaction; all LMO's are titanium−terminal hydrogen interactions, or three center, two electron Ti−H−Ti interactions. Figure 7a shows a localized molecular orbital corresponding to one of the three center, two electron bonds in the C_{2h} structure, and Figure 7b shows a plot of the total electron density in this isomer. The total density plot shows ample evidence of a H−Ti−H bridging bond even though, as noted above, the Ti−H distance is considerably longer than is seen in an ordinary bonding situation. Figure 8a shows the localized molecular orbital corresponding to the three center bond in the C_s plane in the structure $C_s(1)$. Plots of the total density can be seen in Figure 8b, (i) and (ii). Three center, two electron bonding is clear here as well. There is some distortion of the three center bonds, due to the unequal numbers of terminal hydrogens on the two titanium centers. There is clearly more electron density betwen the bridging hydrogens and the titanium with only two terminal hydrogens (the titanium center on the left), producing a short bond/long bond arrangement in the bridges.

Calculated Mulliken charges for the C_{2h} (Figure 2b) and $C_s(1)$ (Figure 2c) isomers are shown in Table 3. Mulliken charges

(24) Edmiston, C.; Ruedenberg, K. *Rev. Mod. Phys.* **1963**, *35*, 457.

Table 3. Mulliken Charges Calculated Using the MP2 Density (Comparable Basis Sets Were Used: TZVP(f) for Ti_2H_8 and TZVP(d) for B_2H_6)

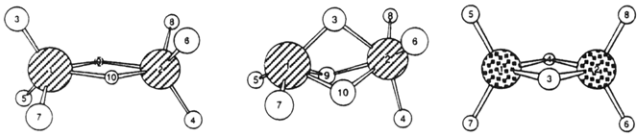

C_{2h} $C_s(1)$ D_{2h}

Ti_2H_8		B_2H_6
C_{2h}	$C_s(1)$	D_{2h}
Ti(1) 0.498	Ti(1) 0.308	B(1) −0.150
H(3) −0.143	Ti(2) 0.394	H(3) 0.105
H(5) −0.111	H(3) −0.107	H(5) 0.022
H(9) −0.131	H(4) −0.133	
	H(5) −0.106	
	H(6) −0.141	
	H(9) 0.016	

for diborane (B_2H_6) calculated with an equivalent basis set to that used for Ti_2H_8 are also shown for comparison. According to the Mulliken charges diborane has little ionic character (of course this is open to debate: Cioslowski and McKee[23b] use a Bader type analysis and conclude that B_2H_6 is "quite ionic"). The Ti_2H_8 isomers exhibit a higher degree of bond polarization (although the out-of-plane Ti−H−Ti interactions in $C_s(1)$ are much less polar than those for the other bridging bonds seen in Table 3), not surprising considering the difference in the electronegativities of titanium and hydrogen. One may recall that TiH_2 forms a lattice structure in the solid state[25] with a titanium coordination number of 8, so it may be reasonable to think of Ti_2H_8 as a precursor which, if given the opportunity, would react with other titanium and hydrogen atoms (or indeed other titanium hydride molecules) to form extended polymeric structures.

(d) Calculated IR Frequencies. Vibrational frequencies were calculated at the MP2/TZVP level for all minima and transition states found. Those calculated for the C_{2h} (Figure 2b) and $C_s(2)$ (Figure 2d) isomers were chosen for comparison with experiment.

In Margrave's matrix isolation experiment[9] one may expect to observe co-existence of species which would not occur in an unhindered environment. We therefore expect that the presence of Ti_2H_8 dimers should not preclude the presence of TiH_4.

The experimental frequency assigned to a Ti−H stretch in TiH_4 is 1658 cm^{-1}; the calculated Ti−H stretch frequency for TiH_4 is 1788 cm^{-1}. The calculated Ti−H stretch frequency may be scaled to the experimental one by a factor of 0.93. This scaling factor is applied to all calculated frequencies to account for basis set deficiencies and higher order correlation effects.

Vibrational frequencies can be seen in Table 4. The scaled calculated frequencies can be compared to the experimental frequencies observed by Margrave.[9] Although definite assignments are difficult, there are a number of features of the spectra which are *highly consistent* with the presence of hydrogen-bridged compounds. Firstly, there is a broad intense feature centered on 1490 cm^{-1} in the experimental spectrum. This coincides nearly exactly with the most intense calculated frequency (scaled) for the C_{2h} isomer (1487 cm^{-1}). Furthermore, a broad intense feature between 1300 and 1500 cm^{-1} is considered indicative of a bridge stretch in a double hydrogen bridged compound,[26] and the normal mode of the calculated

(25) Greenwood, N. N.; Earnshaw, A. In *Chemistry of the Elements*; Pergamon Press, 1984; pp 73.

(26) Marks, T. J.; Jolb, J. R. *Chem. Rev.* **1977**, *77*, 272.

Table 4. Calculated Harmonic Vibrational Frequencies for the Ti_2H_8 Isomers C_{2h} and $C_s(2)$[a]

sym	vibration	freq/ cm^{-1}	scaled freq/ cm^{-1}	intensity/ km mol^{-1}	exptl freq[9]/ cm^{-1}
			C_{2h}		
Bu	$H_t$bend	382.5	355.7	128.9	
Bu	$H_t$bend	489.0	454.8	138.2	
Au	$H_t$bend	547.0	508.7	179.7	
Bu	Ti−H_{br} str	1599.0	1487.1	2706.2	1490 broad
Bu	Ti−H_t str	1785.4	1660.4	951.1	1658
Au	Ti−H_t str	1789.3	1664.0	547.1	1665
			$C_s(2)$		
A′	$H_t$bend	382.3	355.5	138.6	
A″	$H_{t,br}$bend	481.4	447.7	138.0	
A′	$H_t$bend	495.8	461.1	157.7	
A′	$H_t$bend	526.4	489.5	113.7	
A′	$H_t$bend	571.4	531.4	297.6	
A′	H_{br}bend	1162.5	1081.1	193.4	1140 broad
A′	H_{br}bend	1340.4	1246.6	100.2	
A′	Ti−H_{br} str	1655.0	1539.1	1405.3	1515
A′	Ti−H_t str	1738.5	1616.8	381.5	1620
A″	Ti−H_t str	1747.7	1625.4	257.9	
A′	Ti−$H_{t,br}$ str	1762.4	1639.0	130.0	
A″	Ti−H_t str	1763.1	1639.7	442.8	1645
A′	Ti−H_t str	1771.0	1647.0	108.6	

[a] Scaling factor of 0.93 used. Only calculated frequencies with an intensity greater than 100 km/mol are reported.

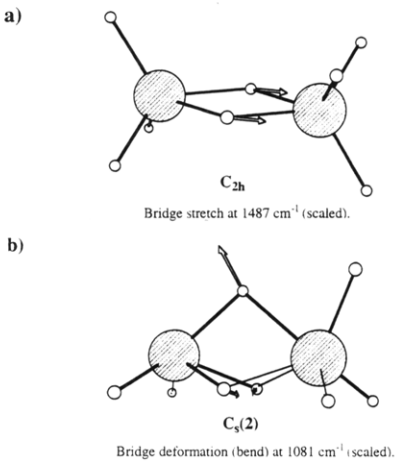

Figure 9. (a) Normal mode of the calculated frequency (1487 cm^{-1} (scaled) that corresponds with a broad feature centered at 1490 cm^{-1} in the experimental spectrum. (b) Normal mode of the calculated frequency at 1081 cm^{-1} (scaled). This may correspond to the experimental peak found at 1140 cm^{-1}.

frequency is in fact a bridge stretch (Figure 9a). Secondly, there is a smaller peak in the spectrum centered at 1140 cm^{-1} and a corresponding calculated frequency (scaled) at 1081 cm^{-1}. There is a discrepancy here of ~60 cm^{-1} but Kaupp and Schleyer have noted that considerable differences between calculations and matrix experiments for soft bending modes are expected due to interactions between guest and host molecules.[27] Features in this region are known to be indicative of a bridge deformation in three bridging hydrogen species,[26] and the calculated frequency does correspond to a bridging hydrogen bend in the $C_s(2)$ isomer (Figure 9b).

The most intense calculated frequency for the $C_s(2)$ isomer (at 1539 cm^{-1}) may correspond to a feature seen at 1515 cm^{-1} in the spectrum (Margrave labels this peak Ti_xH_2), and the presence of a triplet centered at 1658 cm^{-1} may be explained by the slightly different environments encountered by different terminal hydrogens in the bridging compounds. This is sup-

(27) Kaupp, M.; Schleyer, P. R. *J. Am. Chem. Soc.* **1993**, *115*, 11202.

ported by the scaled calculated Ti−H stretch frequencies at 1640, 1660, and 1664 cm^{-1}.

Of course, even though the calculated frequencies are consistent with Margrave's spectrum, to establish the presence of dimers beyond doubt would require a matrix isolation experiment with annealing and monitoring of corresponding changes in peak intensity such as those Andrews and co-workers have performed on magnesium and beryllium hydrides.[28] This is necessary as although there is a large thermodynamic driving force and no barrier to dimerization low mobility in a matrix experiment may inhibit the process.

IV. Summary and Conclusions

TiH_4 is found to dimerize with no barrier and a large thermodynamic driving force (up to 46 kcal mol^{-1} on the classical potential energy surface) producing both doubly hydrogen bridged and triply hydrogen bridged Ti_2H_8 isomers. The potential energy surface of Ti_2H_8 is very flat, suggesting continuous rapid interconversion between $(\mu\text{-H})_2$ and $(\mu\text{-H})_3$ isomers and also between rotational isomers. It is conceivable that interaction with host molecules in a matrix isolation experiment could hinder this interconversion process.

Inclusion of dynamic electron correlation in calculations is essential to produce both reliable geometries and energetics. The effect of dynamic electron correlation is especially large for the $(\mu\text{-H})_3$ isomers. Nonetheless, a crucial result is that all bridging structures are found to be quite stable relative to the separated monomers, *even at the Hartree−Fock level of theory*. This is very likely due to the fact that unlike CH_4 and SiH_4, TiH_4 cannot be thought of as a saturated molecule. Thus, the impact of the s^2d^2 electronic configuration of titanium versus the s^2p^2 electronic configuration of carbon and silicon has a spectacular effect on the structure and energetics of the titanium hydrides investigated in this study. The well-known ability of titanium to accommodate more than four ligands is obviously essential to the formation of the Ti_2H_8 dimers. The electron deficiency of titanium in TiH_4, that is its desire to fill its available d orbitals, is likely the main driving force in the dimerization of TiH_4. In this sense, titanium is a transition metal analog of the electron deficient main group element boron. A desire for higher titanium coordination numbers can also be seen in the energetic preference for triple bridged structures over double bridged structures.

The bonding in the Ti_2H_8 isomers appears to be polar in character with electrostatic attraction between positively charged titanium centers and negatively charged hydrogens. This suggests that the polarized $Ti^{\delta+}-H^{\delta-}$ bonds in TiH_4 have some role to play in the preference for the dimeric Ti_2H_8 species.

Calculated infrared frequencies are consistent with the spectra produced by a matrix isolation experiment on titanium hydrides done by Margrave et al. However, further experimental work is needed to establish without doubt the presence of dimers.

Although different terminal substituents such as chlorine and cyclopentadienyl may have some affect on the system, the large thermodynamic driving force for dimerization with bridging hydrogens seen in this study must have some role to play in systems such as the titanocene dimer and $(\eta^5\text{-}C_5H_5)_2TiBH_4$ which contain bridging hydrogens and one or more titanium centers.

Acknowledgment. This work was supported by a grant from the National Science Foundation (CHE-9317317) and by the Division of Chemical Sciences, Office of Basic Energy, USDOE, via the Ames Laboratory. The calculations reported here were performed on IBM RS 6000 workstations generously provided by Iowa State University and on the CRAY-MP and CRAY C-90 computers at the San Diego Supercomputer Center. The authors thank Dr. Michael Schmidt and Mr. Jan Jensen for several informative discussions.

JA950569D

(28) (a) Tague, T. J.; Andrews, L. *J. Phys. Chem.* **1994**, *98*, 8611. (b) Tague, T. J.; Andrews, L. *J. Am. Chem. Soc.* **1993**, *115*, 12111.